RESEARCH ACTIVITIES VIII
Laser Research Center for Molecular Science

VIII-A Developments and Researches of New Laser Materials

Although development of lasers is remarkable, there are no lasers which lase in ultraviolet and far infrared regions. However, it is expected that these kinds of lasers break out a great revolution in not only the molecular science but also in the industrial world.

In this project we research characters of new materials for ultraviolet and far infrared lasers, and develop new lasers by using these laser materials.

VIII-A-1 Ce^{3+}:$LiCaAlF_6$ Crystal for High-Gain or High-Peak-Power Amplification of Ultraviolet Femtosecond Pulses and New Potential Ultraviolet Gain Medium: Ce^{3+}:$LiSr_{0.8}Ca_{0.2}AlF_6$

LIU, Zhenlin[1]; KOZEKI, Toshimasa; SUZUKI, Yuji; SARUKURA, Nobuhiko; SHIMAMURA, Kiyoshi[2]; FUKUDA, Tsuguo[2]; HIRANO, Masahiro[1]; HOSONO, Hideo[1,3]
([1]ERATO; [2]Tohoku Univ.; [3]Tokyo Inst. Tech.)

[*IEEE J. Sel. Top. Quantum Electron.* **7**, 542 (2001)]

To develop high-peak-power ultrashort pulse laser systems in the ultraviolet region, a large Ce^{3+}:$LiCaAlF_6$ (Ce:LiCAF) crystal, a tunable ultraviolet laser medium with large saturation fluence and broad gain spectrum width, was grown successfully with a diameter of more than 70 mm. To demonstrate high small signal gain, a four-pass confocal amplifier with 60 dB gain and 54 mJ output energy was constructed. Chirped pulse amplification (CPA) in the ultraviolet region was demonstrated using Ce:LiCAF for higher energy extraction. A modified bow-tie-style four-pass amplifier pumped by 100-mJ 266-nm 10-Hz pulses from a Q-switched Nd:YAG laser had 370-times gain and delivered 6-mJ 290-nm pulses. After dispersion compensation, the output pulses can be compressed down to 115 fs. This is the first ultraviolet, all-solid-state high-peak-power CPA laser system using ultraviolet gain media, and this demonstration shows further scalability of the Ce:LiCAF CPA system. Additionally, a new gain medium, Ce^{3+}:$LiSr_{0.8}Ca_{0.2}AlF_6$, with longer fluorescence lifetime and sufficient gain spectrum width over 18 nm was grown to upgrade this system as a candidate for a final power amplifier gain module.

VIII-A-2 Optical Fiber for Deep Ultraviolet Light

OTO, Masanori[1]; KIKUGAWA, Shinya[2]; SARUKURA, Nobuhiko; HIRANO, Masahiro[3]; HOSONO, Hideo[3,4]
([1]Showa Electric Wire Cable; [2]Asahi Glass Co. Ltd.; [3]ERATO; [4]Tokyo Inst. Tech.)

[*IEEE Photonics Technol. Lett.* **13**, 978 (2001)]

Deep ultraviolet optical fibers are fabricated using modified SiO_2 glasses containing 2000-ppm fluorine for the clad and 200 ppm for the core. The transmission at 193 nm is improved to more than 60%/m by optimizing the fiber drawing condition. The H-2-impregnation into the fiber suppresses the degradation of the transmission by irradiation of ArF excimer laser (50 mJ/cm^2/pulse). Further improvement may be expected by reducing oxygen-deficient center (I) defect generation in the drawing process.

VIII-A-3 Crystal Growth of Fluorides for Optical Applications

SHIMAMURA, Kiyoshi[1]; SATO, Hiroki[1]; BENSALAH, Amina[1]; SUDESH, Vikas[1]; MACHIDA, Hiroshi[2]; SARUKURA, Nobuhiko; FUKUDA, Tsuguo[1]
([1]Tohoku Univ.; [2]Tokin Corp.)

[*Cryst. Res. Technol.* **36**, 801 (2001)]

Ce-doped and undoped $LiCaAlF_6$, $LiSrAlF_6$, $LiYF_4$, $LiLuF_4$ and $KMgF_3$ single crystals were grown by the Czochralski technique under CF_4 atmosphere. The effective distribution coefficients of Ce^{3+} in $LiCaAlF_6$, $LiSrAlF_6$, $LiYF_4$ and $LiLuF_4$ were determined to be 0.031, 0.028, 0.116 and 0.054, respectively. Laser output energy of 60 mJ and 27 mJ were obtained using the grown Ce:$LiCaAlF_6$ and Ce:$LiLuF_4$ single crystals, respectively. Undoped $LiCaAlF_6$ and $KMgF_3$ single crystals showed a transmission edge at 112 nm and 115 nm, respectively.

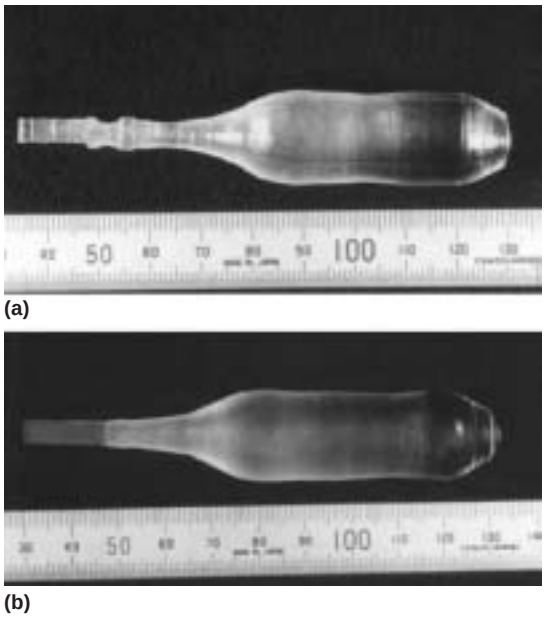

Figure 1. As-grown Ce-doped (a) $LiCaAlF_6$ and (b) $LiSrAlF_6$ single crystals 18 mm in diameter pulled along the *a*-axis.

VIII-A-4 Growth of Ce-Doped Colquiriite- and Scheelite-Type Single Crystals for UV Laser Applications

SHIMAMURA, Kiyoshi[1]; SATO, Hiroki[1]; BENSALAH, Amina[1]; MACHIDA, Hiroshi[2]; SARUKURA, Nobuhiko; FUKUDA, Tsuguo[1]
([1]Tohoku Univ.; [2]Tokin Corp.)

[*Opt. Mater.* **19**, 109 (2002)]

Ce-doped Colquiriite- and Scheelite-type fluoride single crystals were grown by the Czochralski technique. The formation of inclusions and cracks accompanying the crystal growth was investigated. The effective distribution co-efficients of Ce^{3+} in $LiCaAlF_6$, $LiSrAlF_6$, $LiYF_4$ and $LiLuF_4$ were determined to be 0.031, 0.028, 0.116 and 0.054, respectively. Ultraviolet pulse generations with an output energy of 60 and 27 mJ were obtained from Ce:$LiCaAlF_6$ and Ce:$LiLuF_4$ lasers.

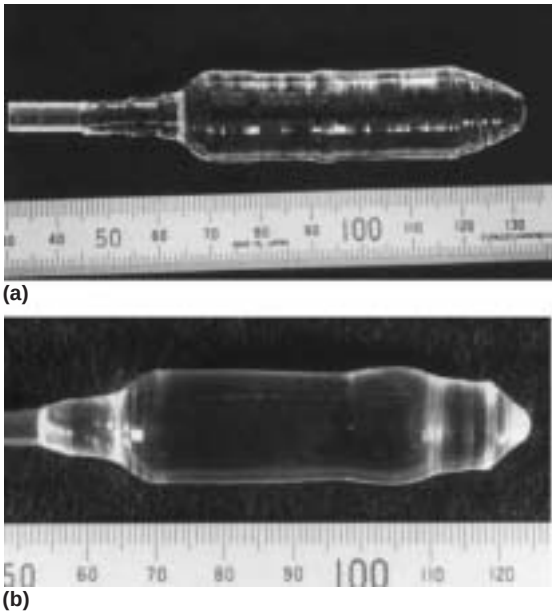

Figure 1. As-grown Ce-doped: (a) $LiYF_4$ and (b) $LiLuF_4$ single crystals of 18 mm in diameter pulled along the *a*-axis.

VIII-A-5 High-Energy Pulse Generation from Solid-State Ultraviolet Lasers Using Large Ce:Fluoride Crystals

LIU, Zhenlin[1]; SHIMAMURA, Kiyoshi[2]; FUKUDA, Tsuguo[2]; KOZEKI, Toshimasa; SUZUKI, Yuji; SARUKURA, Nobuhiko
([1]ERATO; [2]Tohoku Univ.)

[*Opt. Mater.* **19**, 123 (2002)]

A large Ce^{3+}:$LiCaAlF_6$ (Ce:LiCAF) crystal with 15 mm diameter was grown successfully by the Czochralski method. Owing to its large size, 60 mJ, 289 nm pulses were generated directly from a quasi-coaxially pumped Ce:LiCAF laser. In addition, a new noncollinear Brewster-angle-pumping disk oscillator scheme was demonstrated for further output-energy scaling. An ultraviolet solid-state Ce^{3+}:$LiLuF_4$ (Ce:LLF) laser which was pumped transversely by a KrF excimer laser with the repetition rate of 1 Hz produced a 27 mJ, 309 nm pulse using a large Ce:LLFcrystal which was grown by the Czochralski method, and the slope efficiency was approximately 17%.

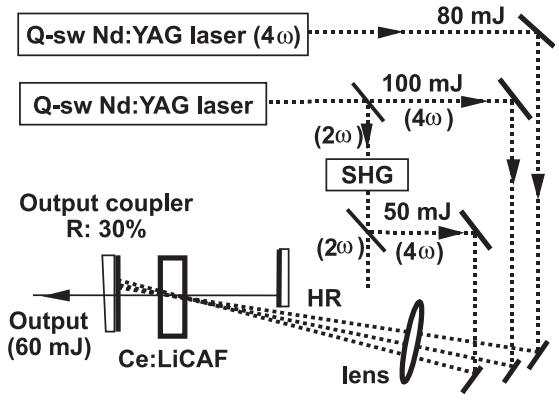

Figure 1. Experimental setup for high-power Ce:LiCAF laser pumped by the fourth harmonics of two Q-switched Nd:YAG lasers.

VIII-A-6 New Adjustment Technique for Time Coincidence of Femtosecond Laser Pulses Using Third Harmonic Generation in Air and its Application to Holograph Encoding System

KAWAMURA, Ken-ichi[1]; ITO, Naoko[2]; SARUKURA, Nobuhiko; HIRANO, Masahiro[1]; HOSONO, Hideo[1,3]
([1]ERATO; [2]Mater. Struct. Lab.; [3]Tokyo Inst. Tech.)

[*Rev. Sci. Instrum.* **73**, 1711 (2002)]

The third harmonic generation of light (266 nm) is enhanced, sensitively depending on the time delay between a pair of pulses split from a single 800 nm femtosecond laser pulse, when they are focused and collided in air. This finding offers a convenient and widely applicable technique to detect temporal and spatial overlapping of two femtosecond pulses. This technique has several advantages over the conventional sum frequency generation method using nonlinear optical crystals, since it obviates the need for expensive crystals, free from phase matching, and elimination of temporal walk off. By applying it to "a holographic encoding system using an interference femtosecond laser pulse," a periodic fringe spacing is minimized to ~ 430 nm by extending the colliding angle between two-pulse beams up to ~ 160 ºC.

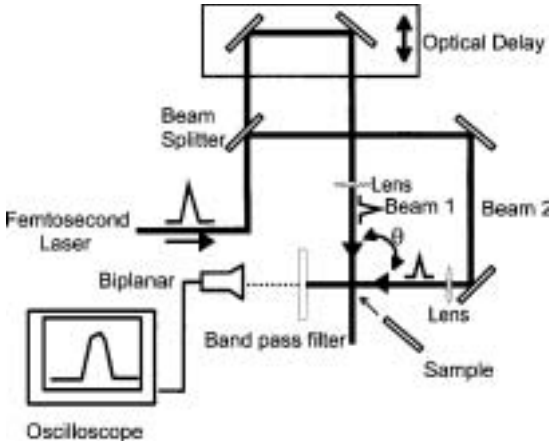

Figure 1. Experimental setup for holographic encoding system.

VIII-A-7 Hybrid Time-Resolved Spectroscopic System for Evaluating Laser Material Using a Table-Top-Sized, Low-Jitter, 3-MeV Picosecond Electron-Beam Source with a Photocathode

SUZUKI, Yuji; KOZEKI, Toshimasa; ONO, Shingo; MURAKAMI, Hidetoshi; OHTAKE, Hideyuki; SARUKURA, Nobuhiko; NAKAJYO, Terunobu[1]; SAKAI, Fumio[1]; AOKI, Yasushi[1]
([1]Sumitomo Heavy Industries, Ltd.)

[*Appl. Phys. Lett.* **80**, 3280 (2002)]

Hybrid time-resolved spectroscopy of laser media comparing electron-beam excitation and optically excited cases is performed using a newly developed, table-top-sized, low-jitter, 3-MeV picosecond electron-beam source with a photocathode. The properties of an electron-beam-pumped Ce^{3+}:$LiCaAlF_6$ (Ce:LiCAF) ultraviolet laser medium significant differ from those of an optically pumped medium.

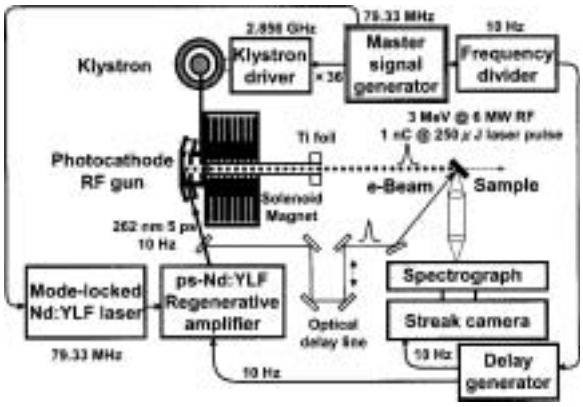

Figure 1. Experimental setup. The photocathode rf gun was irradiated with 262-nm optical pulses from a Nd:YLF regenerative system synchronously operated with a 2.856-GHz, 6-MW klystron to accelerate the extracted 1-nC photoelectron beam. The e-beam was irradiated onto the sample after being passed through titanium foil. A portion of the pumping optical pulse irradiated the same sample to compare the excitation scheme. A streak camera was equipped with a 30-cm spectrograph to measure the fluorescence spectrum and fluorescence lifetime.

VIII-A-8 Simultaneous Measurement of Thickness and Water Content of Thin Black Ink Films for the Printing Using THz Radiation

OHTAKE, Hideyuki; SUZUKI, Yuji; ONO, Shingo; SARUKURA, Nobuhiko; HIROSUMI, Tomoya[1]; OKADA, Tomoaki[2]
([1]AISIN SEIKI Co., Ltd.; [2]Mitsubishi Heavy Industry Co., Ltd.)

[*Jpn. J. Appl. Phys., Part 2* **41**, L475 (2002)]

Using THz radiation, a simple, noncontact, simultaneous method is applied to measure thickness and water content of black ink films independently from frequency-dependent and frequency-independent absorption characteristics of black ink films.

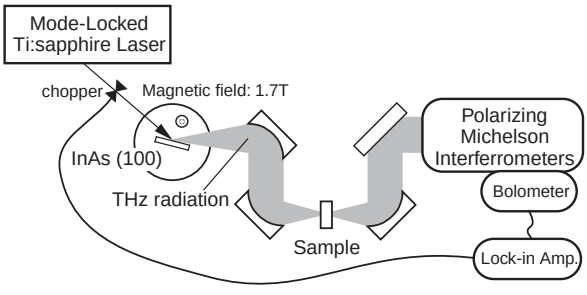

Figure 1. Experimental setup for simultaneously measuring thickness and water content of thin black ink films. The magnetic field direction is from the back to the surface.

VIII-A-9 Far-Infrared Absorption Measurements of Polypeptides and Cytochrome *c* by THz Radiation

YAMAMOTO, Kohji[1]; TOMINAGA, Keisuke[1]; SASAKAWA, Hiroaki[1]; TAMURA, Atsuo[1]; MURAKAMI, Hidetoshi; OHTAKE, Hideyuki; SARUKURA, Nobuhiko
([1]Kobe Univ.)

[*Bull. Chem. Soc. Jpn.* **75**, 1083 (2002)]

Pulsed terahertz (THz) radiation and black-body radiation are applied to measure far infrared (FIR) absorption spectra of polypeptides and cytochrome *c* in the wavenumber region from 7 cm^{-1} to 160 cm^{-1}. In the region from 7 cm^{-1} to 55 cm^{-1}, FIR absorption cross sections of polyglycine and poly-*L*-alanine in powder are greater than those of glycine and *L*-alanine in powder. On the other hand, FIR absorption spectra of cytochrome *c* in lyophilized powder show little dependence on protein structures. The structures of biopolymers are investigated by mid-IR absorption (polypeptides and cytochrome *c*) and by resonance Raman scattering (cytochrome *c*). FIR spectral features of biopolymers in the THz frequency region are qualitatively discussed in terms of density of states and homogeneous/inhomogeneous broadening.

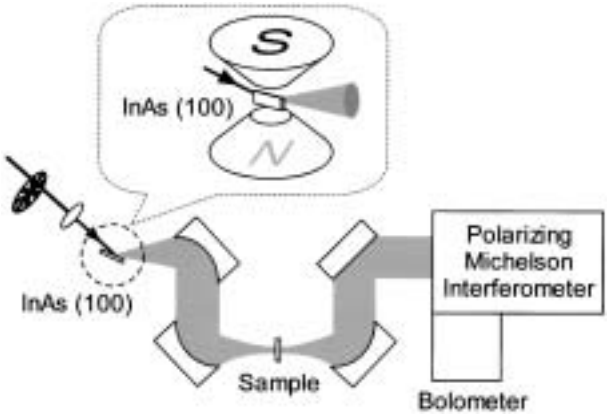

Figure 1. FIR absorption spectrometer using the THz radiation. Pulses at 800 nm with 70-fs width at 80-MHz repetition rate irradiate an InAs wafer, which is placed in a magnetic flux density of 1.7 T generated by an electromagnet. The (100)-InAs surface is parallel to a direction of the magnetic flux density. The THz radiation from the (100)-InAs is collimated by an off-axes parabolic mirror. The THz radiation is focused at a sample position and collimated again by an off-axes mirror. Intensity of the THz radiation is detected by a germanium bolometer which is cooled by helium liquid. Chopping frequency of the pump pulse is 200 Hz. A polarizing Michelson interferometer is vacuumsealed. All the FIR absorption system other than the polarizing Michelson interferometer is open to air. When using the black-body radiation for FIR absorption measurements, the generation part of the THz-radiation is replaced by a black-body.

VIII-A-10 0.43 J, 10 Hz Fourth Harmonic Generation of Nd:YAG Laser Using Large $Li_2B_4O_7$ Crystals

SUZUKI, Yuji; ONO, Shingo; MURAKAMI, Hidetoshi; KOZEKI, Toshimasa; OHTAKE, Hideyuki; SARUKURA, Nobuhiko; MASADA, Genta[1]; SHIRAISHI, Hiroyuki[1]; SEKINE, Ichiro[1]
([1]Mitsubishi Materials Corp.)

[*Jpn. J. Appl. Phys., Part 2* **41**, L823 (2002)]

Using large-sized $Li_2B_4O_7$ crystals, 0.43 J, 266 nm pulses are obtained from a 10 Hz Nd:YAG laser with a total conversion efficiency of 30.5%. Moreover, 4 W operation for over 15 h is demonstrated.

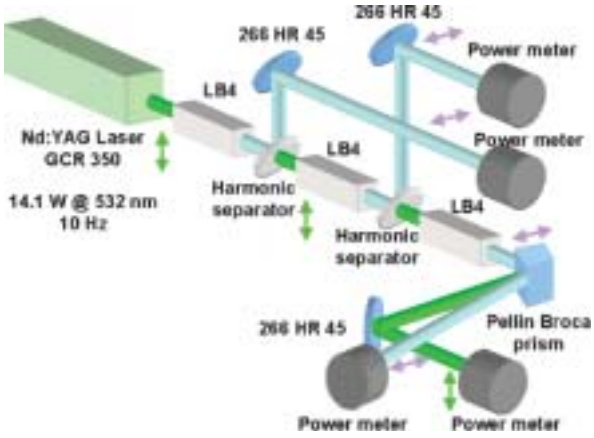

Figure 1. Experimental setup for three-cascade, fourth harmonic generation using LB_4 crystals.

VIII-A-11 Electron-Beam Excitation of a Ce^{3+}:$LiCaAlF_6$ Crystal for Future High-Peak-Power UV Lasers

KOZEKI, Toshimasa; SUZUKI, Yuji; SAKAI, Masahiro; OHTAKE, Hideyuki; SARUKURA, Nobuhiko; SHIMAMURA, Kiyoshi[1]; FUKUDA, Tsuguo[1]; NAKAJYO, Terunobu[2]; SAKAI, Fumio[2]; AOKI, Yasushi[2]
([1]Tohoku Univ.; [2]Sumitomo Heavy Industries Ltd.)

[*Appl. Phys. B* **74**, S185 (2002)]

In this experiment, we performed ultrafast spectroscopy on an electron-beam-excited Ce^{3+}:$LiCaAlF_6$ (Ce:LiCAF) crystal. The time-resolved fluorescence spectrum and lifetime with e-beam pumping differ significantly from those in the optically pumped case. These results suggest a new pumping scheme for an ultrashort pulse amplifier.

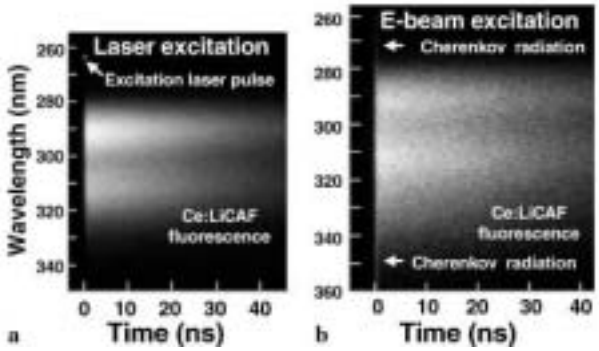

Figure 1. The streak camera images of the fluorescence from Ce:LiCAF, excited **a** by a 262-nm-pulse and **b** by an electron pulse. In the case of electron pulse excitation, a broadband, short-duration Cherenkov radiation is clearly seen.

VIII-B Development and Research of Advanced Tunable Solid State Lasers

Diode-pumped solid-state lasers can provide excellent spatial mode quality and narrow linewidths. The high spectral power brightness of these lasers has allowed high efficiency frequency extension by nonlinear frequency conversion. Moreover, the availability of new and improved nonlinear optical crystals makes these techniques more practical. Additionally, quasi phase matching (QPM) is a new technique instead of conventional birefringent phase matching for compensating phase velocity dispersion in frequency conversion. These kinds of advanced tunable solid-state light sources, so to speak "Chroma Chip Lasers," will assist the research of molecular science.

In this projects we are developing Chroma Chip Lasers based on diode-pumped-microchip-solid-sate lasers and advanced nonlinear frequency conversion technique.

VIII-B-1 Thermal-Birefringence-Induced Depolarization in Nd:YAG Ceramics

SHOJI, Ichiro; SATO, Yoichi; KURIMURA, Sunao; LUPEI, Voicu[1]; TAIRA, Takunori; IKESUE, Akio[2]; YOSHIDA, Kunio[3]

([1]IMS and IAP, Romania; [2]JFCC; [3]Osaka Inst. Tech.)

[*Opt. Lett.* **27**, 234 (2002)]

Nd:YAG ceramics are promising candidates for high-power and high-efficiency microchip laser materials because highly transparent and highly Nd^{3+}-doped samples are available[1)] without degradation in thermomechanical properties.[2)] We have investigated the optical properties of Nd:YAG ceramics and succeeded in microchip laser oscillation.[3)] In this work we have investigated depolarization effect caused by thermally induced birefringence in Nd:YAG ceramics, which should be an essential issue for controlling polarization under high-power operation.

Thermal birefringence effect was measured with the pump-probe experiment. A Ti:sapphire laser oscillating at 808 nm was used as the pump source, which was focused onto the sample with the radius of 80 μm. The linearly polarized He-Ne laser beam of 1 mm radius was used as the probe. After passing through the sample, only the depolarized component of the probe beam was detected. The measured samples were 1.0, 1.3, 2.0, and 3.4 at.% Nd^{3+}-doped YAG ceramics, and 1.0 and 1.3 at.% Nd:YAG single crystals. The thickness of each sample was ~ 1 mm, and (111)-cut samples were used for the single crystals.

Figure 1 shows the depolarization as a function of Nd^{3+} concentration at the absorbed pump power of 1000 mW. We found that the depolarization is nearly same between the ceramic and single-crystal YAG for the same Nd^{3+} concentrations. Because YAG ceramics consist of a lot of YAG single-crystal grains (their sizes are in several tens of microns) with various directions, which means that the birefringence effect in a ceramic sample is average of that in those grains, we suppose our results indicate that the average is close to the birefringence effect for (111)-cut Nd:YAG single crystals.

Moreover, it was also found that the depolarization became larger in samples with higher Nd^{3+} concentrations even if the same pump power was absorbed. We believe that the main reason is the difference of thermal loading for the samples with different Nd^{3+} concentrations. For a highly Nd^{3+}-doped sample, in which the interaction between Nd^{3+} ions is significant, the amount of nonradiative relaxation increases and radiative quantum efficiency gets smaller. Under the condition of no laser extraction, the smaller quantum efficiency causes larger thermal loading, that is, more heat generation in the sample even at the same absorbed power, and this induces larger thermal birefringence. The dotted line in Figure 1 shows the calculated result, in which we used the values of thermal loading obtained by Lupei *et al.*[4)] The agreement between the experiment and rough estimation is satisfactory. When lasing occurs, on the other hand, thermal birefringence is expected to be greatly reduced because the thermal loading is then independent of radiative quantum efficiency. This means that *cw* or high-repetition-rate, high-average-power Q-switched operation is preferable for highly Nd^{3+}-doped ceramics.

References

1) A. Ikesue, T. Kinoshita, K. Kamata and K. Yoshida, *J. Am. Ceram. Soc.* **78**, 1033 (1995).
2) T. Taira, A. Ikesue and K. Yoshida, *OSA Trends in Optics and Photonics* **19**, 430 (1998).
3) I. Shoji, S. Kurimura, Y. Sato, T. Taira, A. Ikesue and K. Yoshida, *Appl. Phys. Lett.* **77**, 939 (2000).
4) V. Lupei, A. Lupei, N. Pavel, T. Taira, I. Shoji and A. Ikesue, *Appl. Phys. Lett.* **79**, 590 (2001).

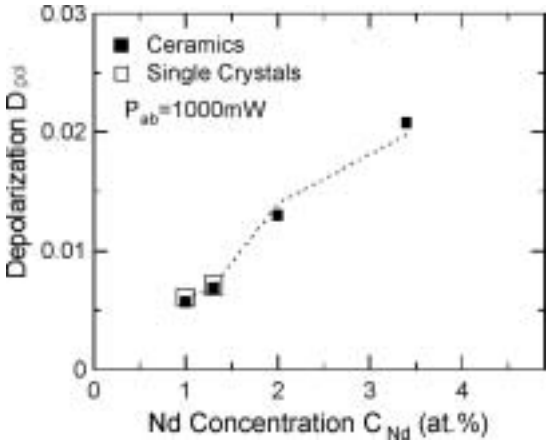

Figure 1. Depolarization as a function of Nd^{3+} concentration for the ceramic and single-crystal samples at the absorbed pump power of 1000 mW. The dotted line is the calculation taking account of increase of thermal loading.

VIII-B-2 Intrinsic Reduction of the Depolarization Loss in Solid-State Lasers by Use of a (110)-Cut $Y_3Al_5O_{12}$ Crystal

SHOJI, Ichiro; TAIRA, Takunori

[*Appl. Phys. Lett.* **80**, 3048 (2002)]

Thermally induced birefringence in solid-state laser materials is a serious problem in developing high-power and high-beam-quality lasers and amplifiers because it causes bifocusing and depolarization of a linearly polarized beam. A number of techniques which use a 90o rotator and a quarter-wave plate, *etc.*, have been suggested to compensate the depolarization. However, these compensations have been applied exclusively for (111)-cut YAG crystals, presumably because the (111) plane has simple, circularly symmetrical birefringence so that using (111)-cut rods is conventional. We report intrinsic reduction of depolarization without any compensation by use of Nd:YAG rods cut other than (111).

Koechner and Rice analyzed thermally induced birefringence in Nd:YAG rods with various directions,[1),2)] and concluded that the amount of depolarization at the high-power limit is independent of rod directions, as shown in Figure 1. However, there were two mistakes in their theory. Figure 1 also shows the dependence of the depolarization on absorbed pump power based on our calculation when the laser beam radius r_a is equal to the rod radius r_0. The amount of depolarization depends on the directions of planes and polarizations even at high power, and becomes smallest when the angle between the direction of polarization and the crystal axis, γ, is equal to 45˚ in the (100) plane, the amount for which is half that for the (111) plane at high power and 1/6 at low power.

Moreover, we have found that the depolarization can be greatly reduced by use of a (110)-cut rod under condition that r_a is smaller than r_0. When the distance from the center of the rod, r, is as large as r_0, the eigenvectors are directed nearly to the radial and the tangential directions at all the angles. On the other hand, when r is small, all eigenvectors are nearly aligned in one direction. Because of this nature, if the direction of the polarization is close to the crystal axis, a beam with small radius can propagate through the rod almost undepolarized. Figure 2 shows, as an example, dependence of the depolarization on the absorbed pump power when $r_a = r_0/5$ and $\gamma = 0$˚. The depolarization for the (110) plane reduces to about 1/50 of that for the (111) plane. This condition can be realized by use of an aperture to control the beam size in the case of the uniform pumping. A composite material in which the doped YAG is surrounded by the undoped YAG also makes the same condition and realizes better extraction efficiency. For the end pumping, on the other hand, the condition is easily satisfied because the focused pump beam itself plays a role as a gain aperture.

References

1) W. Koechner and D. K.Rice, *J. Quantum Electron* **QE-6**, 557 (1970).
2) W. Koechner and D. K. Rice, *J. Opt. Soc. Am.* **61**, 758 (1971).

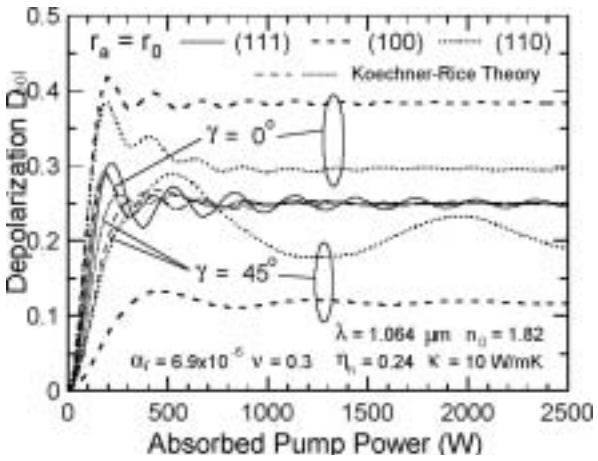

Figure 1. Dependence of the depolarization on the absorbed pump power for the (111), (100), and (110) planes based on Koechner and Rice's theory (thin curves) and our calculation (thick curves).

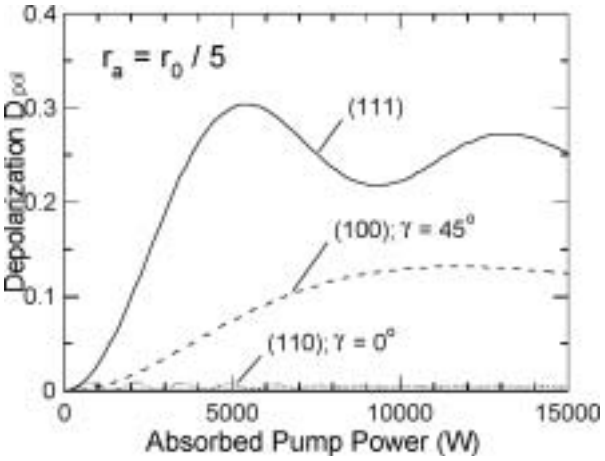

Figure 2. Dependence of the depolarization on the absorbed pump power for the (111), (100), and (110) planes when $r_a = r_0/5$.

VIII-B-3 The Effect of Nd Concentration on the Spectroscopic and Emission Decay Properties of Highly-Doped Nd:YAG Ceramics

LUPEI, Voicu[1]; LUPEI, Aurelia[1]; GEORGESCU, Serban[1]; TAIRA, Takunori; SATO, Yoichi; IKESUE, Akio[2]
([1]IAP-NILPRP, Romania; [2]JFCC)

[*Phys. Rev. B* **64**, 092102 (2001)]

The renewed interest in the use of highly concentrated Nd:YAG laser materials for constructing solid state lasers rises important questions concerning the effect of Nd concentration (C_{Nd}) on the spectroscopic and emission decay characteristics that determine the performances of these lasers. Highly doped Nd:YAG components can be produced by various techniques such as crystal growth by the Thermal Gradient Technique,[1)] flux,[2)] epitaxial thin film deposition[3)] or ceramic techniques.[4)] Despite of the fact that some of these components have been used in laser experiments, no detailed account of the effect of C_{Nd} on their spectros-

copic and emission decay properties has been reported. This work reports the results of spectroscopic and emission decay investigations of Nd:YAG ceramics with up to 9-at.% Nd.

High optical quality transparent Nd:YAG ceramics have been produced by the technique described in Reference 4). The high-resolution transmission spectra were measured at temperatures between 10 and 300 K by using a high-resolution (better than 0.3 cm^{-1}) one-meter double monochromator. For the emission decay a photon counting technique of 20-ns resolution was used and the excitation was made non-selectively at room temperature with the 2nd harmonic of a Q-switched Nd:YAG laser (10-nsec pulse width). The intensity of excitation was kept low in order to avoid a high population of the emitting level $^4F_{3/2}$ (under ~1%) that could favor upconversion by excited state absorption or energy transfer.

The transmission spectra of Nd:YAG ceramic samples of 1-at.% Nd are similar to those of single crystals[5] of the same C_{Nd}. No obvious line shifts or broadenings have been observed in any spectral range in agreement with previous investigations on 1-at.% Nd:YAG ceramics.[6] With increasing Nd concentration the positions of the spectral lines remain practically unchanged with very slight shifts for some of the optical transitions and with a selective broadening. The structures of the satellites in the low-temperature high-resolution spectra at 1-at.% Nd do not contain any additional satellites with respect to those reported in single crystals,[5] showing that no additional defects in the vicinity of the Nd ions occur. The only major satellites in the transmission spectra of the Nd:YAG ceramics are those connected with crystal-field perturbations inside of statistical ensembles of Nd^{3+} ions sitting on near lattice sites. At low Nd concentrations the most important of such ensembles are Nd ion pairs: the satellites corresponding to the first (*n.n.*)- and second (*n.n.n.*)- order pairs are clearly resolved in most of the optical transitions (satellites M_1, spectral shift up to 5 to 6 cm^{-1} and M_2, shift up to 2 to 3 cm^{-1}, respectively), as shown in Figure 1 for the transition $^4I_{9/2}(Z_1) \rightarrow {}^2P_{1/2}$ at various Nd concentrations. With increasing of C_{Nd} the relative intensities of the pair lines increase, while the ones of the isolated ions decrease. Moreover, at very high concentrations, new satellites T, whose relative intensities increase with C_{Nd} faster than those of the pairs, show up. Most likely these new satellites are connected with triads of Nd^{3+} ions on near lattice sites, the larger spectral shift being consistent with the expected larger mutual crystal-field perturbation inside of these ensembles.

The weakly excited emission decay at room temperature is accelerated and shows departures from exponentials with increasing C_{Nd} (as shown in Figure 2) The decay can be divided into four successive temporal regions: (i) a very sharp drop that terminates practically within the first two microseconds of the decay and whose extent on the intensity scale increases almost proportionally to C_{Nd}; (ii) a quasi-exponential portion that blurs at high C_{Nd}; (iii) a non-exponential dependence; (iv) a new quasi-exponential dependence. The border between these regions is not sharp and the transition is gradual. The extent of the regions (ii) and (iii) reduces with increasing C_{Nd}: the region (iv) is not seen in the decay of the diluted samples during 6–8 e-foldings of low noise decay at the low pump intensities used in this experiment. The emission quantum efficiency η_{qe} in the presence of energy transfer can be then determined. It decreases with increasing C_{Nd} and all the excitation lost non-radiatively by cross-relaxation is transformed into heat. This limits the possibilities of using concentrated Nd:YAG components in laser emission regimes implying the storage of excitation energy (the Q-switched regime). However, these materials show good prospect to be used in continuous-wave regimes, where the effect of the reduction of η_{qe} with increasing C_{Nd} on the threshold can be compensated by an enhanced absorption of the pump radiation.

References

1) Y. Zhou, *J. Crystal Growth* **78**, 31 (1986).
2) P. Gavrilovic, M. S. O'Neill, J. H. Zarabi, J. E. Williams, W. H. Grodkiewics and B Bruce, *Appl. Phys. Lett.* **65**, 1820 (1994).
3) D Pelenc, B. Chambaz, I Chartier, B. Ferrand and J. C. Vial, *J. Phys. (France) IV* **1**, 311 (1991).
4) A. Ikesue, T. Kinoshita, K. Kamata and K. Yoshida, *J. Am. Ceram. Soc.* **78**, 1033 (1995).
5) V. Lupei, A. Lupei, C. Tiseanu, S. Georgescu, C. Stoicescu and P. Nanau, *Phys. Rev. B* **51**, 8 (1995).
6) M. Sekita, H. Haneda, T. Yanagitani and S. Shirasaki, *J. Appl. Phys.* **67**, 453 (1990).

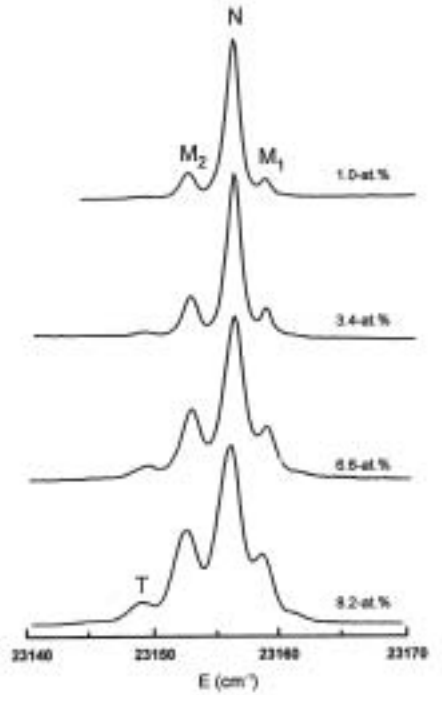

Figure 1. $^4I_{9/2} \rightarrow {}^2P_{1/2}$ transmission spectra for different concentrations at low temperature.

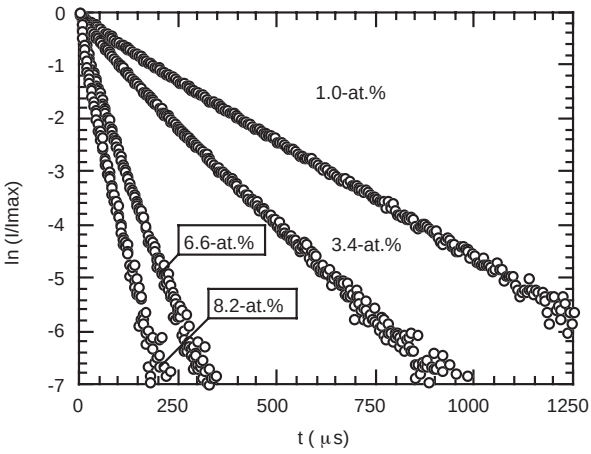

Figure 2. $^4F_{3/2}$ emission decays for Nd:YAG ceramics of different concentrations at room temperature.

VIII-B-4 Spectroscopy and Laser Emission under Hot Band Resonant Pumping in Highly Doped Nd:YAG Ceramics

LUPEI, Voicu[1]; TAIRA, Takunori; LUPEI, Aurelia[1]; PAVEL, Nicolaie; SHOJI, Ichiro; IKESUE, Akio[2]
([1]IAP-NILPRP, Romania; [2]JFCC)

[*Opt. Commun.* **195**, 225 (2001)]

Owing to important thermo-mechanical properties, such as hardness, high thermal conductivity and high stress-fracture limit as well as to its fairly good spectroscopic properties (four-level laser scheme, high emission cross-section, fairly long lifetime), Nd:YAG remains a material of choice for the construction of solid-state lasers. However, the inability of the conventional growth techniques for bulk single-crystals (Czochralski) to incorporate Nd concentrations (C_{Nd}) above 1.2–1.4 at.% without a serious deterioration of the optical and structural properties, together with the sharp and relatively weak absorption lines at these concentrations limit the use of these crystals both in the direction of the high power lasers and of very efficient microchip lasers. This paper investigates the spectroscopic properties and the emission dynamics of Nd^{3+} ions in highly concentrated Nd:YAG ceramics. The implication of these properties on the laser emission is discussed and illustrated with the 1064-nm emission under hot band resonant pump in the emitting level.

The samples under study are Nd:YAG ceramics with Nd concentrations up to 9-at.%, produced as described in Reference 1). The main techniques of investigation are the high spectral resolution optical transmission and the high temporal resolution emission decay. The laser emission was investigated on samples of up to 3.8-at.% Nd under Ti:Sapphire laser end-pumping.

The transmission spectra at room temperature enable the selection of optical transitions suitable for diode laser pumping. A very promising such transition could be the doubly-peaked band centered around 885 nm made up by the hot bands $Z_2 \rightarrow R_1$ and $Z_3 \rightarrow R_2$ of the absorption $^4I_{9/2} \rightarrow {}^4F_{3/2}$. Our measurements show that the absorption coefficients of the two peaks of the 885-nm band are approximately equal at room temperature and become appreciable at high values of C_{Nd}: they increase from ~ 1.7 cm^{-1} at 1-at.% Nd to ~ 6.5 cm^{-1} at 4-at.% and 13 to 14 cm^{-1} at 9-at.% Nd, while the FWHM increases from ~2.5 nm at 1-at.% Nd to ~3.2 nm at 9-at.% Nd, very suitable for diode laser pumping.

The room temperature global emission decay under low intensity non-selective pump of Nd:YAG ceramic samples show C_{Nd}-dependent departures from exponential.[2)] The quantum efficiency η_{qe}, which was determined as a function of C_{Nd} by using the energy transfer parameters obtained from the emission decay, is shown in Figure 1. This dependence is different from that used traditionally $\eta_{qe} = [1 + C_{Nd}/C_0]^{-1}$, which is based on a C^2_{Nd}-dependence of the transfer function at all Nd concentrations, but is in a very good agreement with the reported data on quantum efficiency,[3)] fractional thermal load[4)] and pump-induced birefringence.[5)] These results indicate that the concentrated Nd:YAG ceramics show potential for construction of efficient CW solid state lasers.

The CW 1064-nm laser emission potential of the concentrated Nd:YAG ceramics was investigated under resonant pump in $^4F_{3/2}$ level at 885-nm in an end-pump laser configuration. The Nd concentration of the laser active component was 3.8-at.%; the quantum efficiency η_{qe} was ~ 0.32, leading to a figure of merit $\eta_{qe}C_{Nd}$ of 1.21 and to a calculated product $\eta_{qe}\tau_D$ of ~ 83 μsec. The uncoated plane parallel 1.5-mm thick active component was placed in a 25-mm plane-concave resonator with a 50-mm radius output coupler. The end pumping was made with a Ti:sapphire laser focused on the sample in a 160-μm diameter spot. The emission power versus the absorbed power is represented in Figure 2. For a 5% transmission output coupler the threshold of emission in absorbed power was ~ 65 mW and the slope efficiency ~ 40%, and at 500-mW absorbed power the laser emitted in excess of 167-mW in a beam with a M^2 factor equal to 1.61.6. Analysis of these data shows that for a given output coupler transmission T, the threshold and the slope efficiency can be consistently described by using the same value of the global loss parameter $(T + L)\eta_B^{-1}$, where η_B is the superposition factor of the laser mode and the pump volumes and L represents all the other losses, including the residual Fresnell loss at the wavelength of emission. This global loss parameter amounts to 0.10.005 for $T = 0.05$ and 0.045 ± 0.002 for $T = 0.01$; these two values are consistent with a superposition factor of ~ 0.73, in agreement with the measured ratio of the laser emission and the pump beam diameters, and with a loss parameter $L = 0.023$.

In conclusion the laser emission of a 3.8-at.% Nd ceramic laser component under hot band resonant pump at 885-nm with a Ti:sapphire laser is demonstrated. The laser active component used in this experiment is the most concentrated Nd:YAG active component reported to lase at 1064 nm. The performances of this laser could be improved by using coated active components of higher optical quality.

References

1) A. Ikesue, T. Kinoshita, K. Kamata and K. Yoshida, *J. Am. Ceram. Soc.* **78**, 1033 (1995).
2) V. Lupei, A. Lupei, S. Georgescu, T. Taira, Y. Sato and A.

Ikesue, *Phys. Rev. B* **64**, 092102 (2001).
3) K. K. Deb, R. G. Buser and J. Paul, *Appl. Opt.* **20**, 1203 (1981).
4) T. Y. Fan, *IEEE J. Quantum Electron.* **29**, 1457 (1993).
5) I. Shoji, Y. Sato, S. Kurimura, T. Taira A. Ikesue and K. Yoshida, *Advanced Solid State Lasers Conference*, Seattle-USA, Jan. 2001, paper ME14.

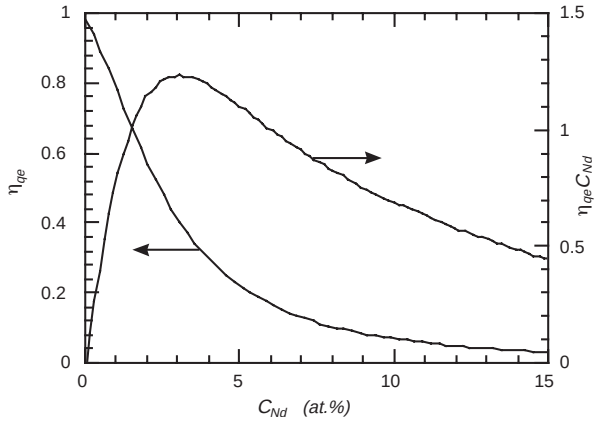

Figure 1. Calculated concentration dependence of emission quantum efficiency η_{qe} and of $\eta_{qe}C_{Nd}$ parameter.

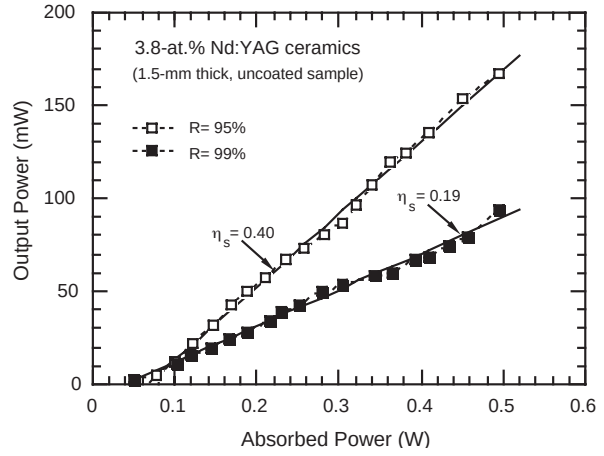

Figure 2. Output power function of absorbed power for an uncoated 3.8-at.% Nd:YAG ceramics sample under 885-nm end pumping by Ti:sapphire laser.

VIII-B-5 Efficient Laser Emission in Concentrated Nd Laser Materials under Pumping into the Emitting Level

LUPEI, Voicu[1]; PAVEL, Nicolaie[2]; TAIRA, Takunori
([1]IAP-NILPRP, Romania; [2]IMS and IAP-NILPRP, Romania)

[*IEEE J. Quantum Electron.* **38**, 240 (2002)]

The enhancement of overall efficiency, low transverse-mode laser emission in miniature lasers, and scaling to high powers are among the most important directions in the development of solid-state lasers. The first of these implies an increase of slope efficiency and a reduction of emission threshold; the second relies on increased absorption of the pump while the third imposes the reduction on heat generation. A suitable choice of the laser material, with optimised spectroscopic and thermo-mechanical properties, of the optical pumping scheme or of the laser design is then crucial. There is no laser material to fulfill optimally all these requirements and thus the choice is limited within well-defined segments of performance.

The present paper shows that a means to overcome weak pump absorption on transitions directly to the $^4F_{3/2}$ level in the diluted (~ 1-at.%) Nd laser-materials is to increase the Nd concentration (C_{Nd}). The use of concentrated Nd laser materials requires the examination of several important basic aspects such as the state of Nd ions in YAG samples produced by various techniques, and the effect of C_{Nd} on the spectroscopic and population dynamics properties, in order to select new transitions suitable for pumping and to determine the range of C_{Nd} adequate for laser emission. The Nd:YAG ceramic samples used in this investigation have up to 9-at.% Nd and were supplied by the Japan Fine Ceramics Center, Nagoya, Japan, while the Nd:YAG crystals (2.4 and 3.5-at.%) and Nd:YVO_4 crystals (1, 2, and 3-at.%) were purchased.

The pumping at 885 nm in Nd:YAG reduces the quantum defect with respect to the 808-nm pumping into $^4F_{5/2}$ by about 30% in the case of 1064-nm emission and by ~58% for 940-nm emission, thus contributing to a considerable reduction in the fractional thermal load. Thus, the near degeneracy of the $Z_2 \rightarrow R_1$ and $Z_3 \rightarrow R_2$ absorption lines could be useful for the occurrence of absorption bands suitable for direct diode laser pumping into the $^4F_{3/2}$ state. This near degeneracy takes place in many Nd laser materials and it could help to get more efficient or more powerful emission even from laser active components with good spectroscopic characteristics but poorer thermo-mechanical properties. In the case of Nd:YVO_4, no accidental degeneracy of the thermally-activated transitions occurs. However, for this material the absorption line $Z_1 \rightarrow R_1$ at 879.8 nm has a FWHM similar to the traditional pump transition $Z_1 \rightarrow {}^4F_{5/2}(1)$ at 808.6 nm, while the peak absorption coefficient is only 40–50% smaller. This reduction can be easily compensated by an increase in C_{Nd}. Thus in the case of Nd:YVO_4, the transition $Z_1 \rightarrow R_1$ of the $^4I_{9/2} \rightarrow {}^4F_{3/2}$ absorption can be used for direct pumping into the emitting level, leading to a reduction of the quantum defect with respect to 808.6-nm pump by 27.4% in the case of 1064-nm $^4F_{3/2} \rightarrow {}^4I_{11/2}$ emission and by 65.6% for 915-nm $^4F_{3/2} \rightarrow {}^4I_{9/2}$ emission.

For Nd:YVO_4 the effects of the energy transfer on the emission decay are very poorly characterized and an analysis similar to YAG[1,2] is not possible at the present time. However, the investigation of emission decay in Nd:$GdVO_4$ (a crystal similar with YVO_4) gives energy transfer parameters about two times larger than in Nd:YAG.[3] Moreover, the investigation of the pump intensity effect on laser emission in Nd:YVO_4 concludes that the up-conversion processes by energy transfer in this crystal are much stronger than in Nd:YAG.[4] Thus, a stronger decrease of emission quantum efficiency with increased C_{Nd} in Nd:YVO_4 could be expected, although figures of merit $\eta_{qe}C_{Nd}$ larger than for 1-at.% Nd doping could be still obtained for a certain range of higher C_{Nd}.

The 1064-nm laser emission in concentrated

Nd:YAG ceramics and single crystals and in Nd:YVO_4 crystals is investigated using oscillators end pumped by Ti:sapphire laser. Figure 1a shows the laser output power function of the absorbed power for the Nd:YAG ceramic laser components. The most concentrated component to lase under 885-nm pumping was a 0.4-mm thick sample of 6.8-at.% Nd: for the 95% output mirror the slope efficiency (versus the absorbed power) was 20% with the emission threshold of 144 mW. For a 1.5-mm thick 3.8-at.% Nd sample and a 95% output coupler reflectivity the slope efficiency was 42%, the threshold of emission was 58 mW and the output power reaches in excess of 132 mW for 350 mW absorbed pump with a laser beam M^2 factor of 1.6 × 1.6. The highest slope of 51% was obtained for the output mirror of 90% reflectivity, but with an increased threshold pump power of 115 mW. The laser output power versus the absorbed power for uncoated 2.4-at.% (3.0-mm thick) and 3.5-at.% (1.0-mm thick) Nd:YAG crystals under 885-nm pumping is shown in Figure 1b, in comparison with those of a standard 1-at.% (3.0-mm thick) Nd component. For the 1-at.% Nd:YAG sample the slope efficiency was 0.54 and the threshold absorbed power was 31 mW. A deterioration of these parameters with increasing C_{Nd} was observed: while for the 2.4-at.% Nd:YAG crystal the slope efficiency was 0.50 and the absorbed power at threshold was 45 mW, for the 3.5-at.% Nd:YAG sample the slope efficiency decreased to 0.46 with a threshold absorbed power of 65 mW. Figure 2 presents the laser performances for 0.9-mm thick Nd:YVO_4 components of 1, 2, and 3-at.% Nd under 879.8-nm pumping in the configuration *E*//*c*-crystal axis and with the 95% reflectivity output coupler. In spite of using uncoated active elements the laser parameters obtained with the 1-at.% Nd sample are substantially improved (slope efficiency of 70% and absorbed pump power at threshold of 21 mW) with respect to those reported in Reference 5) for a thicker sample. For the 2-at.% Nd component the threshold of emission in absorbed power was 44 mW, the slope efficiency reached 67% and for 420-mW absorbed power the laser emitted 265 mW at 1064 nm. A slope efficiency of 58% and a threshold of 58 mW absorbed power were determined for the 3-at.% Nd:YVO_4 sample. The residual losses *L* were determined as ~0.005, 0.01 and ~0.016 for the 1, 2, and 3-at.% Nd:$YAVO_4$ crystals, respectively.

In conclusions, the investigation of the effect of Nd concentration on emission decay of Nd:YAG indicates that up to quite high concentrations the reduction of the emission quantum efficiency by self-quenching can be compensated by the increase of pump absorption. Efficient CW laser emission is demonstrated under direct pumping into the $^4F_{3/2}$ emitting level of Nd:YAG crystals with up to 3.5-at.% Nd, Nd:YAG ceramics with up to 6.8-at.% Nd, and Nd:YVO_4 crystals with up to 3-at.% Nd. Superior performance as compared to traditional pumping into the $^4F_{5/2}$ state were obtained. It is inferred that direct pumping into the emitting level of concentrated Nd materials can improve the efficiency of solid-state lasers in the free-generation or low-storage regimes and opens the possibility of scaling these lasers to high powers.

References

1) V. Lupei, A. Lupei, S. Georgescu, T. Taira, Y. Sato and A. Ikesue, *Phys. Rev. B* **64**, 092102 (2001).
2) V. Lupei, A. Lupei, N. Pavel, T. Taira, I. Shoji and A. Ikesue, *Appl. Phys. Lett.* **79**, 590 (2001).
3) V. Ostroumov, T. Jensen, J. P. Meyn, G. Huber and M.A. Noginov, *J. Opt. Soc. Am. B* **15**, 1052 (1998).
4) Y.F. Chen, C.C. Liao, Y.P. Lan and S.C. Wang, *Appl. Phys. B* **70**, 487 (2000).
5) R. Lavi, S. Jackel, Y. Tzuk, M. Winik, E. Lebiush, M. Katz and I. Paiss, *Appl. Opt.* **38**, 7382 (1999).

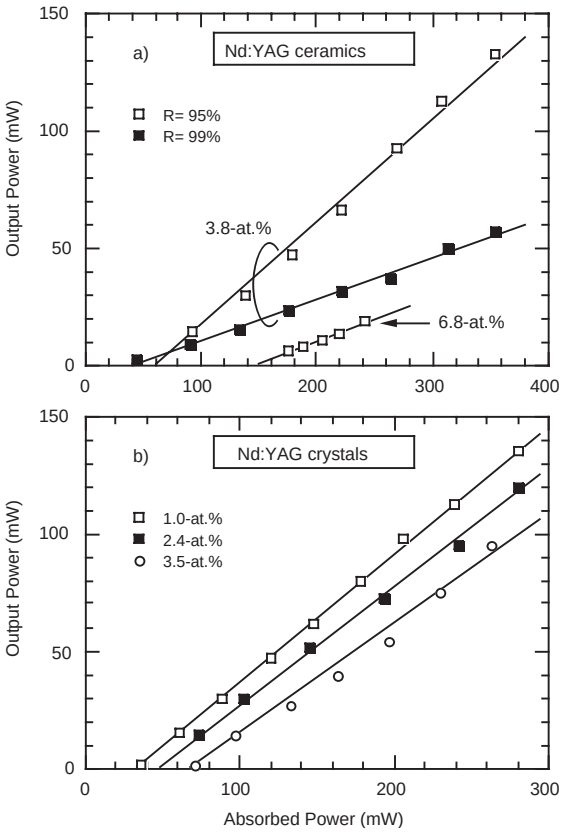

Figure 1. 1064-nm laser emission characteristics for (**a**) uncoated 3.8 and 6.8-at.% Nd:YAG ceramics and for (**b**) uncoated Nd:YAG crystals under 885-nm pumping.

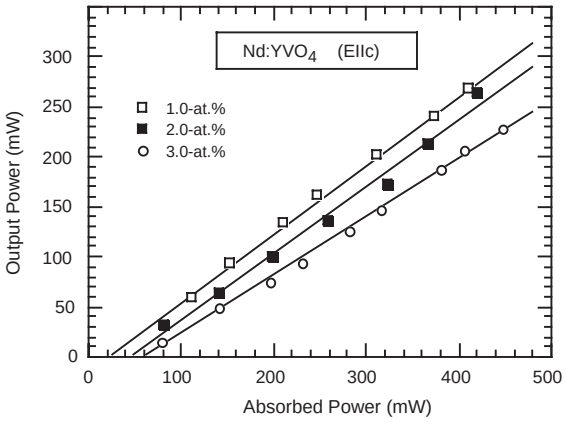

Figure 2. Comparative 1064-nm laser performances for Nd:YVO_4 components under 880-nm pumping (E//c-crystal axis) with a 95% reflectivity output coupler.

VIII-B-6 1064-nm Laser Emission of Highly Doped Nd:Yttrium Aluminium Garnet under 885-nm Diode Laser Pumping

LUPEI, Voicu[1]; PAVEL, Nicolaie[2]; TAIRA, Takunori
([1]IAP-NILPRP, Romania; [2]IMS and IAP-NILPRP, Romania)

[*Appl. Phys. Lett.* **80**, 4309 (2002)]

Owing to the high optical-to-electrical efficiency and to the ability to excite resonantly the energy levels of the laser active ions, the diode laser pumping has a major role in increasing the efficiency of the solid-state lasers. The resonant excitation of Nd^{3+} emission was demonstrated at early stages of laser development by exciting Nd:$CaWO_4$ directly into the emitting level on the transition $^4I_{9/2}$ (Z_2) → $^4F_{3/2}$ (R_2) by the 880-nm recombination radiation of GaAs diodes.[1)] The first diode laser pumped Nd:YAG lasers in transverse[2)] or longitudinal[3)] pumping configurations used the direct excitation of the emitting level on the 869-nm transition $^4I_{9/2}$ (Z_1) → $^4F_{3/2}$ (R_2). Due to the weak absorption on this transition and to the lack of suitable pump diodes, the 869-nm pumping was soon replaced by the 808-nm pumping into the stronger absorption $^4I_{9/2}$ (Z_1) → $^4F_{5/2}$ (S_1). Unfortunately, this introduces a parasitic upper quantum defect between the pump- and the emitting laser levels that contributes to the reduction of the laser emission parameters and to the generation of heat by non-radiative processes in the pumped laser material.

The pumping into the emitting level of Nd-doped materials has received a renewed attention in the last few years: in case of Nd:YAG successful attempts have been made with diluted (~1-at.% Nd) single crystals under Ti:sapphire or diode laser pumping[4),5)] and with highly-doped ceramics or single crystals[6),7)] under Ti:sapphire pump. This paper demonstrates CW laser emission of highly doped Nd:YAG ceramics (up to 3.5-at.% Nd) and single crystals (up to 3.8-at.% Nd) under 885-nm diode laser pumping. The laser emission of a 2.4-at.% Nd:YAG single crystal passively Q-switched with a Cr^{4+}:YAG saturable absorber under CW diode laser pumping at 885 nm is also reported.

A fiber array packed diode bars FAP-81-16C-800B laser (Coherent Co.) whose output is delivered in a 19-fiber bundle confined within an 800-μm diameter aperture with NA = 0.15 was used as pumping source. With a collimating achromatic lens of 60-mm focal length and a focusing achromatic lens of 50-mm focal length the end face of the fiber bundled was imaged into the laser active components in a 780-μm diameter spot. The laser active components were Nd:YAG single crystals of 1-at.% (3-mm thick), 2.4-at.% (3-mm thick) and 3.5-at.% Nd (1.0-mm thick) and Nd:YAG ceramics of 3.8-at.% Nd (1.5 and 2.5-mm thick), AR coated on both sides for 885 and 1064 nm. A plane-concave resonator of 50 mm length with an output mirror of 0.25-m radius of curvature was used. The active component was placed close to the rear mirror, which was coated HR for 1064 nm and HT for the pumping wavelength.

Figure 1a shows the laser performances for the 2.4-at.% Nd:YAG crystal. The maximum slope efficiency of 0.64 was obtained for a 90% reflectivity output mirror, with a corresponding emission threshold 1.51 W. The slope efficiency and the threshold become 0.62 and 0.87 W for 95% reflectivity and 0.26 and 0.25 mW for 99% reflectivity. The output power obtained with 95% reflectivity output mirror for the laser materials used in this experiment is presented in Figure 1b: the best results, *i.e.* a slope efficiency of 0.67 and 0.71 W absorbed power at threshold, were obtained with the 1.0-at.% Nd:YAG crystal of 3.0-mm thickness. The laser parameters *vs.* incident power reveal the practical advantages of the concentrated materials: for the region close to the maximum operating point, where the diode wavelength is ~ 885 nm, the measured slope efficiency in input power for the 3-mm thick crystals is 0.26 for 1-at.% Nd and 0.43, *i.e.* by 65% larger, for 2.4-at.% Nd. At the same time the emission threshold is by ~ 40 % lower for the second crystal and the absorption efficiency is larger by ~ 75%.

The passive Q-switching regime was investigated with Cr^{4+}:YAG saturable absorber (SA) crystals. A plane-plane resonator with the active medium positioned near the rear mirror and the SA crystal placed closed of the output mirror was investigated. Figure 2 shows the average power *vs.* the absorbed power for a 70-mm length resonator. With a Cr:YAG SA of 90% initial transmission (T_0) and an output mirror of 95% reflectivity an average output power of 0.95 W resulted for 5.2-W absorbed power. The maximum repetition rate was 7.1 kHz with the pulse width 37.5 ns over the entire range of absorbed power: this corresponds to a maximum pulse energy of 134 μJ and ~ 3.6 kW peak power. With a 90% reflectivity output mirror the average power decreases to 0.84 W; the pulse width reduces to 26.5 ns, corresponding to ~ 161-μJ pulse energy and ~6 kW peak power. With a Cr:YAG SA of T_0 = 85% and a 95% reflectivity output mirror the laser emitted max. 0.56-W average power at 3.2-kHz repetition rate: the pulse had 175 μJ energy and 5.6-kW peak power. In spite of using a non-optimised scheme, improved laser characteristics (lower threshold, higher average power and pulse energy) resulted compared with a 1.1-at.% composite Nd:YAG laser passively Q-switched by Cr:YAG under 808-nm diode pumping.[8)]

In conclusion, highly efficient 1064-nm CW laser emission under 885-nm diode pumping in concentrated Nd:YAG crystals (up to 3.5-at.% Nd) and ceramics (up to 3.8-at.% Nd) is reported. First highly doped (2.4-at.%) Nd:YAG laser passively Q-switched by a Cr^{4+}:YAG saturable absorber is demonstrated.

References

1) R. Newman, *J. Appl. Phys.* **34**, 437 (1963).
2) M. Ross, *Proc. IEEE* **56**, 196 (1968).
3) L. J. Rosenkrantz, *J. Appl. Phys.* **34**, 4603 (1972).
4) R. Lavi and S. Jackel, *Appl. Opt.* **39**, 3093 (2000).
5) R. Lavi, S. Jackel, A. Tal, E. Lebiush, Y. Tzuk and S. Goldring, *Opt. Commun.* **195**, 427 (2001).
6) V. Lupei, A. Lupei, N. Pavel, T. Taira, I. Shoji and A. Ikesue, *Appl. Phys. Lett.* **79**, 590 (2001).
7) V. Lupei, N. Pavel and T. Taira, *Opt. Lett.* **26**, 1678 (2001).
8) N. Pavel, J. Saikawa, S. Kurimura and T. Taira, *Jpn. J. Appl. Phys.* **40**, 1253 (2001).

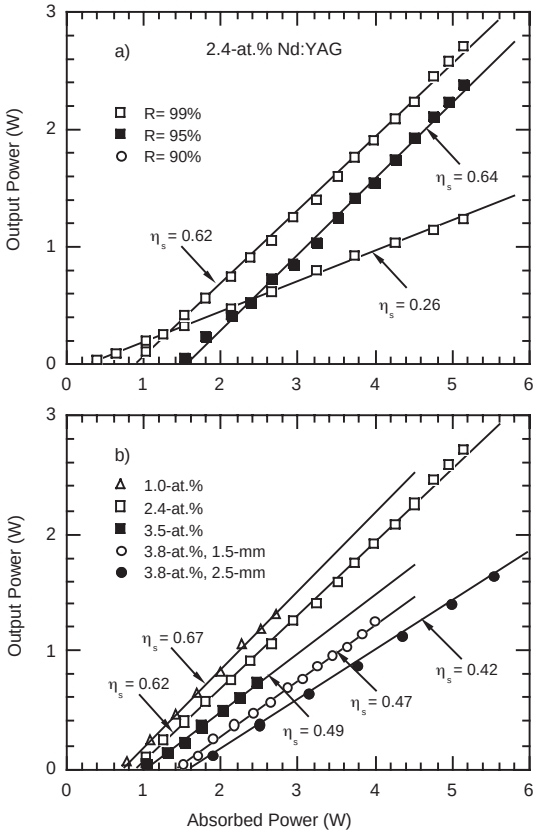

Figure 1. 1064-nm laser emission characteristics for (**a**) a 2.4-at.% Nd:YAG crystal and for (**b**) the Nd:YAG laser active components used in experiments and a 95% reflectivity output mirror under 885-nm diode laser pumping.

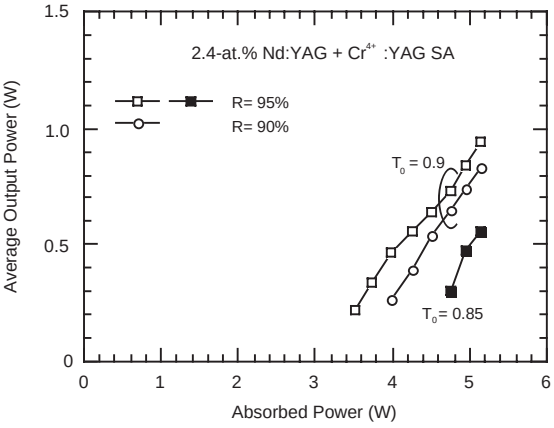

Figure 2. Average output power of a CW diode pumped at 885 nm highly-doped (2.4-at.%) Nd:YAG laser passively Q-switched by Cr^{4+}:YAG saturable absorber.

VIII-B-7 Diode Edge-Pumped Microchip Composite Yb:YAG Laser

DASCALU, Traian; TAIRA, Takunori; PAVEL, Nicolaie

[*Jpn. J. Appl. Phys.* **41**, 606 (2002)]

High power microchip laser based on Yb^{3+} doped materials has been recognized as very useful in the ultrafast-laser field.[1),2)] Thermal effects in the laser gain medium generally limit power scaling of diode-pumped solid-state microchip lasers. Yb:YAG is a gain medium that has improved properties relative to Nd^{3+}-doped gain media[3)] for addressing this issue and efficient room-temperature laser operation (slope efficiency of 65%) has been demonstrated in this material despite the fact that it is a quasi-four-level laser.[4)] Besides of choice of gain medium the configuration that is chosen for pumping, cooling, and extraction plays a critical role in power scaling of microchip laser. Despite of the Yb:YAG low quantum defect, large thermal effects occur at high pumping power. One solution to diminish the thermal lens is to orient the heat flux collinearly with the direction of laser propagation. We propose an edge pumped Yb:YAG microchip scheme. This scheme can be used efficiently only if the pumping power is concentrated into a small region of the microchip consequently a composite material was designed.

The composite material consists in an Yb:YAG core of hexagonal or square shape surrounded by circular shaped undoped YAG. The composite crystal consists of an Yb:YAG doped core surrounded by an undoped YAG region, the core and the undoped crystal being diffusion bonded. The crystal has one side high reflectivity (HR) coated at the laser wavelength and the opposite side anti reflection (AR) coated and it is mounted with its HR coated side on a highly effective micro channel cooling system, Figure 1. Two fiber-coupled diode lasers delivering more than of 100 W at 940 nm are used for pumping. Inside of the microchip the pumping beam propagates by total internal reflection and intersects the Yb:YAG core where it is partially absorbed.

Continuous laser operation was obtained from the 2 at% Yb doped crystal by using an optical resonator of 50-mm length with output coupler of 100-mm radius of curvature and 97% reflectivity output mirror. The slope efficiency for laser operation at more than three times above the threshold is 50% and the laser delivers maximum 1.8 W output power for 5.1 W absorbed power.

In order to evaluate the laser performances under low thermal effects the microchip was operated in quasi-CW mode with a duty factor of 2.5% and 2.4 Hz repetition rate. Figure 2 presents the output *vs.* input power for the 10-at. % doped sample with 97% reflectivity output mirror. Laser emission with 42% slope efficiency and 41-W output peak power at 220-W input power was demonstrated. The experiments show the potential of the microchip laser to be scaled in the range of tens of watts output power.

References

1) C. Honninger, R. Paschotta, M. Graf, F. Morier-Genoud, G. Zhang, M. Moser, S. Biswal, J. Nees, A.Braun, G.A. Mourou, A.Giesen, W. Seeber and U. Keller, *Appl Phys. B* **69**, 3 (1999).

2) C. Honninger, I. Johannsen, M.Moser, G. Zhang, A. Giesen and U. Keller, *Appl.Phys. B* **65**, 423 (1997).

3) L.D.DeLoach, S.A. Payne, L.L. Chase, L.K. Smith, W.L.Kway and W.F. Krupke, *IEEE J. Quantum Electron.* **29**, 1179 (1993).

4) K. Contag, M. Karzewski, C. Stewen, A. Giesen and H. Hugel, *Quantum Electronics* **29**, 697 (1999).

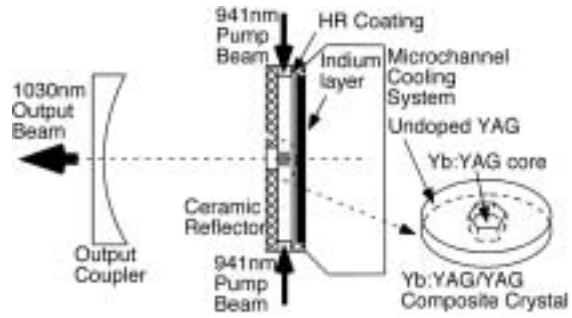

Figure 1. The diode radial-pumped composite Yb:YAG microchip laser.

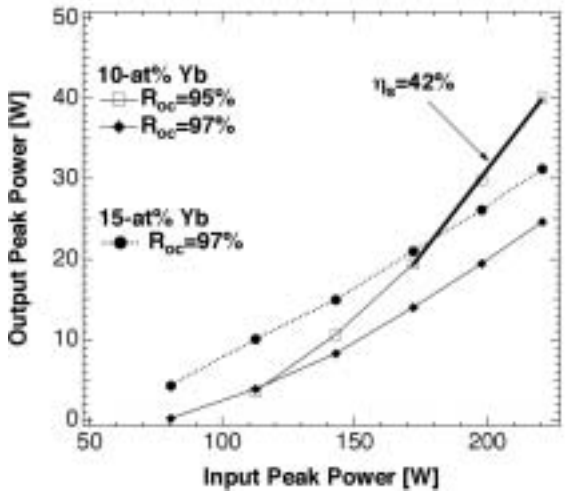

Figure 2. Output power *vs.* input power for quasi CW laser operation for 10-at. % Yb-doping crystal, 2 × 2 mm^2 square core dimensions and 15-at. % Yb-doping crystal, 1.2 × 1.2 mm^2 square core dimensions. Here *R* represents the output mirror reflectivity.